Comparative Study of Short-Circuit Current Contribution from Small Hydropower and DFIG Wind Generators in Power Systems

Doan Kim Tuan

Electrical Faculty, Thai Nguyen University of Technology, Thai Nguyen, Viet Nam

Corresponding Author

DOI: https://dx.doi.org/10.51584/IJRIAS.2025.10100000181

Received: 02 November 2025; Accepted: 10 November 2025; Published: 21 November 2025

ABSTRACT

This paper presents a method for calculating and simulating short-circuit currents in power systems with the simultaneous participation of small hydropower generators and wind power generators based on doubly fed induction machines. Based on detailed modeling of the control structure and power electronic converters, different short-circuit scenarios were established to evaluate the current response of the two generation sources. The simulation results show that the short-circuit current of small hydropower generators exhibits a high initial magnitude and decreases according to the subtransient, transient, and steady-state characteristics. In contrast, the short-circuit current of wind generators using doubly fed induction machines is limited by the converters and protection mechanisms, and is strongly influenced by the applied control strategies. The analysis and comparison of these two generation types accurately reflect the power distribution and current variations in the system during short-circuit conditions. The research results provide an important basis for protection design, reliability assessment, and stable operation of power systems integrating small hydropower and wind energy sources.

Index Terms— DFIG, Control structure, Renewable energy, Short-circuit calculation, Small hydro power plant.

INTRODUCTION

In power system analysis, the calculation and prediction of short-circuit currents play a particularly important role in equipment selection, protection design, and reliability assessment. With today's diverse generation mix, ranging from small hydropower plants to wind turbines employing doubly fed induction generators (DFIG), the characteristics of short-circuit currents have become increasingly complex, requiring specialized analytical methods.

For small hydropower generators, short-circuit currents usually consist of subtransient, transient, and steady-state stages, and are significantly affected by the machine reactances, excitation system parameters, and hydraulic characteristics. Studies have shown that constant switching phenomena and arc voltages during faults must be taken into account to accurately calculate short-circuit currents in hydropower units [3], [4]. In addition, local short-circuit conditions such as inter-turn faults in the stator winding of small hydropower generators are of concern due to their direct impact on equipment safety and lifespan [7]. Furthermore, recent research has analyzed the phenomenon of "hydraulic short-circuit" in hydropower systems, showing that the coupling of hydraulic and electrical processes can lead to highly complex transient behavior [10].

In contrast, the short-circuit response of DFIG-based wind turbines is governed by power electronic converters and protection mechanisms. During faults, DFIGs may sustain or limit current contributions depending on control strategies, reactive power support modes, and the activation of the crowbar circuit [1], [2], [5], [8], [9]. Recent works have developed detailed short-circuit models for DFIGs, considering coordinated control between the rotor-side and grid-side converters [2], as well as the influence of reactive power support strategies on short-circuit current calculations [8]. In particular, new calculation methods have improved the accuracy of short-circuit current prediction for DFIGs, thereby enhancing fault analysis and protection design in power systems [1], [5].

ISSN No. 2454-6194 | DOI: 10.51584/IJRIAS |Volume X Issue X October 2025

In the context of power systems increasingly integrating both small hydropower and DFIG-based wind power, the comparative analysis of short-circuit currents and current responses from these two sources has become essential. This not only supports the development of accurate simulation models but also directly contributes to protection design, operation planning, and improving the reliability of modern power grids [3]–[10].

Based on these considerations, this paper focuses on the system structures of DFIG-based wind turbines and small hydropower generators, and their responses under short-circuit conditions. The next section introduces the control structures of DFIGs and small hydropower generators, together with the short-circuit current calculation methods. Section III provides analyses of the responses of DFIGs and small hydropower units under short-circuit faults, including both transient and sustained cases. The final section presents the conclusions and main findings of the study.

STRUCTURE OF DFIG SYSTEM, SMALL HYDROPOWER, AND SHORT-CIRCUIT CALCULATION METHOD IN POWER SYSTEMS

Control Structure of DFIG-Based Wind Power System

The control structure of a wind power generator using a doubly fed induction generator is established based on the integration of two power electronic converters, namely the rotor-side converter (RSC) and the grid-side converter (GSC), as illustrated in Fig. 1. The rotor-side converter is responsible for controlling the rotor current in the ddd-qqq reference frame, thereby regulating the active and reactive power output of the generator. The grid-side converter ensures a stable DC-link voltage and simultaneously regulates the current exchanged with the power grid [1], [2].

Under normal operating conditions, the rotor-side control system is typically designed using either stator flux orientation (SFO) or grid voltage orientation (GVO), which allows the decoupling of active and reactive power control. Consequently, the DFIG can flexibly meet power dispatch requirements and participate in voltage regulation at the point of common coupling [2], [5].

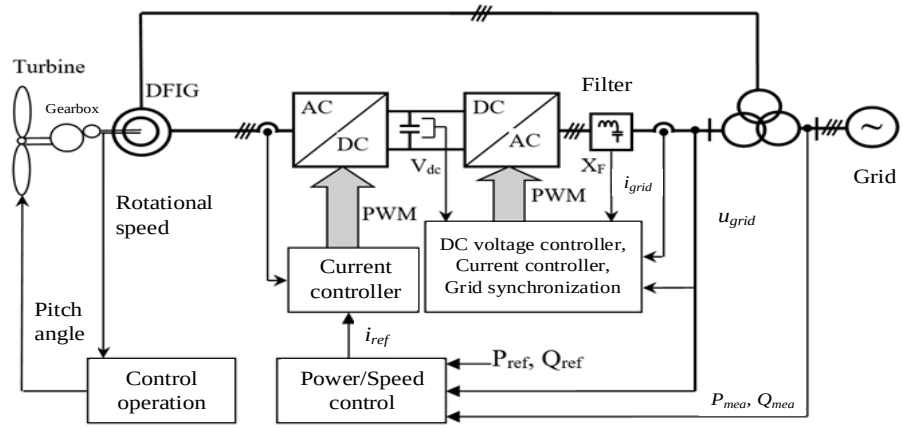

Fig.1 Control structure of DFIG

When a short-circuit occurs in the grid, the short-circuit current characteristics of the DFIG strongly depend on this control structure. If the converters can maintain continuous excitation, the short-circuit current can be limited to a desired level while simultaneously providing reactive power support to the grid [1]. In severe fault conditions, the crowbar protection mechanism is triggered to protect the converters, which alters the fault current characteristics and causes a temporary reduction in controllability. In addition, advanced control strategies, such as emergency reactive power support, have been proposed to improve low-voltage ride-through capability and enhance system stability [8].

Thus, the control structure of the DFIG not only determines the efficiency of operation under normal conditions but also directly influences the current response during short-circuits, playing a key role in fault modeling and short-circuit current calculations.

ISSN No. 2454-6194 | DOI: 10.51584/IJRIAS |Volume X Issue X October 2025

Máy phát thủy điện

The small hydropower generator is a synchronous machine, in which the control system plays a crucial role in maintaining terminal voltage and output power during both normal operation and fault conditions. The Automatic Voltage Regulator (AVR) is responsible for keeping the generator terminal voltage stable by controlling the field current. During short-circuits, the AVR responds rapidly by increasing the excitation current to compensate for the voltage drop, which directly affects the short-circuit current characteristics in the transient stage [3], [4].

In parallel, the Governor regulates the water flow into the turbine, ensuring the balance between mechanical input and electrical output power. In the event of a short-circuit or sudden load change, the Governor responds more slowly than the AVR but is essential for maintaining frequency stability and power output [6]. Furthermore, in systems with stringent stability requirements, a Power System Stabilizer (PSS) can be integrated to provide supplementary signals, helping to damp oscillations and improve the dynamic stability of small hydropower generators [10].

Several studies have also shown that the coordination of AVR, Governor, and PSS significantly influences the transient response of small hydropower generators under fault conditions. For example, during a three-phase short-circuit, the initial current is mainly governed by the machine parameters, while the recovery of voltage and frequency stability largely depends on the control system [6], [7], [10]. In small hydropower plants, the generators are integrated into the grid as illustrated in Fig. 3.

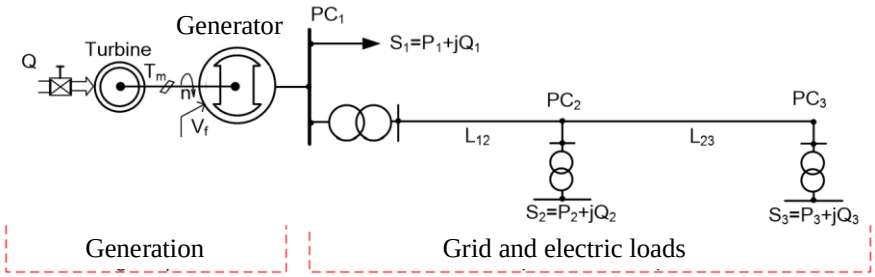

Grid structure

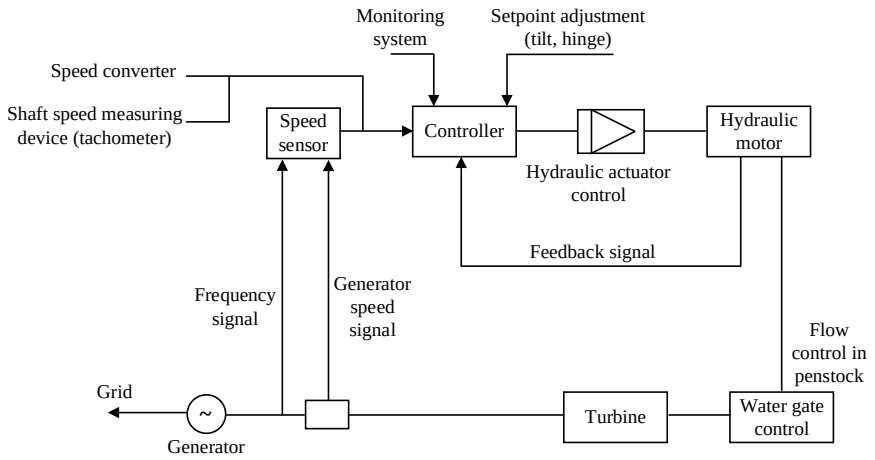

Control structure

Fig.2 Control structure of small hydropower generator

Short-Circuit Calculation Method in Power Systems

Depending on the type of short-circuit, the equivalent circuit diagrams are established using the Thevenin equivalent voltage source at the fault location, as illustrated in the figures below [1]–[6]. In these diagrams, the notation $F^{(3)}$ represents a three-phase short-circuit, $F^{(2)}$ denotes a line-to-line short-circuit, $F^{(1,1)}$ indicates a double line-to-ground short-circuit, and $F^{(1)}$ corresponds to a single line-to-ground short-circuit.

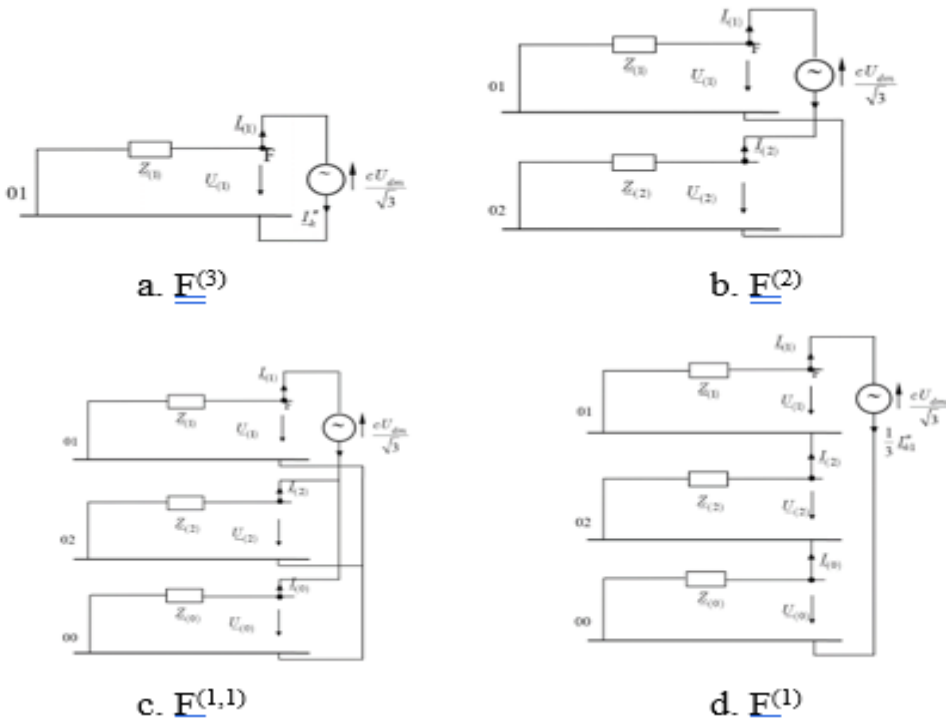

Fig.3 Equivalent circuit for short-circuit calculation

For a three-phase short-circuit: the subtransient short-circuit current and peak short-circuit current at the fault location are given by:

$$I_k^{"} = \frac{cU_n}{\sqrt{3}Z_k} = \frac{cU_n}{\sqrt{3}\sqrt{R_k^2 + X_k^2}} \qquad (1)$$

$$i_p = k_p\sqrt{2}I_k^{"} \qquad (2)$$

where: k_p is the peak factor; c is the coefficient corresponding to the type of power network; U_n is the norminal voltage of the network; R_k and X_k are the resistance and reactance up to the short-circuit location.

For a line-to-line short-circuit [1]–[6]: In the initial stage of the short-circuit current, the negative-sequence impedance is approximately equal to the positive-sequence impedance. The subtransient short-circuit current and peak short-circuit current at the fault location are given by:

$$I_{k2}^{"} = \frac{cU_n}{\left|\dot{Z}_{(1)} + \dot{Z}_{(2)}\right|} = \frac{cU_n}{2\left|\dot{Z}_{(1)}\right|} = \frac{\sqrt{3}}{2}I_k^{"} \qquad (3)$$

$$i_{p2} = k_p\sqrt{2}I_{k2}^{"} \qquad (4)$$

where: $Z_{(1)}$ and $Z_{(2)}$ are the positive-sequence and negative-sequence impedances up to the short-circuit location.

For a double line-to-ground short-circuit [1]–[6]: In the initial stage of the short-circuit current, the negative-sequence impedance is approximately equal to the positive-sequence impedance. If $\dot{Z}_{(2)} = \dot{Z}_{(1)}$, the short-circuit currents in phases B and C are given by:

$$I_{k2Eb}^{"} = cU_n \frac{\left|\dot{Z}_{(0)} / \dot{Z}_{(1)} - \dot{a}\right|}{\left|\dot{Z}_{(1)} + 2\dot{Z}_{(0)}\right|} \qquad (5)$$

$$I_{k2Ec}^{"} = cU_n \frac{\left|\dot{Z}_{(0)} / \dot{Z}_{(1)} - \dot{a}^2\right|}{\left|\dot{Z}_{(1)} + 2\dot{Z}_{(0)}\right|} \qquad (6)$$

ISSN No. 2454-6194 | DOI: 10.51584/IJRIAS |Volume X Issue X October 2025

where: $\dot{a}$ is the rotation operator; $Z_{(0)}$ is the zero-sequence impedance up to the short-circuit location.

The subtransient short-circuit current and peak short-circuit current at the fault location are given by:

$$I''_{kE\,2E} = \frac{\sqrt{3}cU_n}{\left|\dot{Z}_{(1)} + 2\dot{Z}_{(0)}\right|} \quad (7)$$

$$i_{p2E} = k_p\sqrt{2}I''_{k2E} \quad (8)$$

- For a single line-to-ground short-circuit:

If $\dot{Z}_{(2)} = \dot{Z}_{(1)}$, the total subtransient short-circuit current and peak short-circuit current at the fault location are given by:

$$I''_{k1} = \frac{\sqrt{3}cU_n}{\left|2\dot{Z}_{(1)} + \dot{Z}_{(0)}\right|} \quad (9)$$

$$i_{xk1} = k_{xk}\sqrt{2}I''_{k1} \quad (10)$$

IMPACT OF DFIG AND SMALL HYDROPOWER ON SHORT-CIRCUIT CURRENTS

IMPACT OF DFIG ON SHORT-CIRCUIT CURRENTS

Wind generators employing doubly fed induction generators (DFIGs) exhibit short-circuit behavior that is fundamentally different from synchronous generators. During a fault, the short-circuit current of the DFIG is directly governed by the control structure and the load capability of the power electronic converters, rather than being solely dependent on the machine reactances. Several studies have demonstrated that accurate modeling of DFIG short-circuit currents requires consideration of coordinated control between the rotor-side converter (RSC) and grid-side converter (GSC), which allows the fault current characteristics to be correctly represented [1], [2].

Under normal conditions, the rotor-side controller can maintain continuous excitation and provide reactive power support to the grid during a fault, thereby improving voltage recovery [1], [5]. However, under more severe faults, the crowbar protection circuit is activated to safeguard the converters, causing the DFIG to temporarily operate as a squirrel-cage induction generator and thus altering its short-circuit current characteristics [9]. In addition, advanced emergency reactive power support strategies have been proposed to enhance low-voltage ride-through capability, thereby contributing to improved system voltage stability [8].

Therefore, the short-circuit current of a DFIG is not only the result of electromagnetic phenomena within the machine but also the outcome of complex interactions between hardware and control structures. Modern models and calculation methods must therefore integrate the influence of power electronic control systems to accurately reflect the behavior of wind power sources under fault conditions [2], [5], [8].

When a short-circuit occurs in the power system, the response of the DFIG can be described as follows:

Short-term response in the initial transient stage: The grid voltage drops due to the direct stator connection. This leads to large transient currents in both the stator and rotor during the first few cycles. The RSC and GSC are designed to limit the current (typically 1.1–1.2 p.u.). If the current exceeds this threshold, the crowbar circuit is activated, shorting the rotor through a resistor and causing the DFIG to behave like a conventional induction generator [1], [2], [9].

Long-term response: After crowbar activation, the DFIG contributes a decaying short-circuit current over time due to its induction characteristics, with the AC component gradually diminishing [5], [8].

Thus, the short-circuit current contribution of a DFIG follows two scenarios: (i) when the converters limit the current, the short-circuit current contribution remains small; (ii) when the crowbar is activated, the DFIG

contributes a significant short-circuit current similar to an induction generator. The peak current can reach 4–6 p.u immediately after the fault, but this decays over time, typically reducing to about 1.2–1.5 p.u after a few cycles. The contribution of short-circuit current is illustrated in Fig. 4 [2], [9].

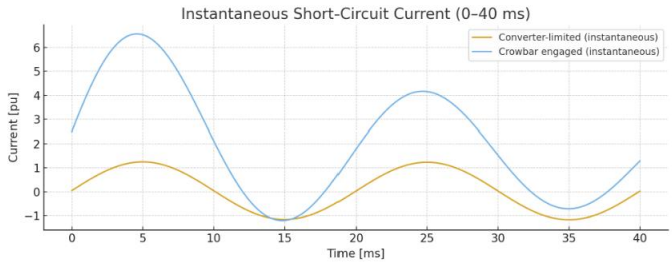

a. Instantaneous short-circuit current

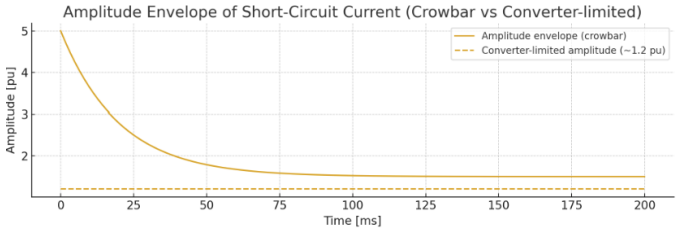

b. Amplitude envelope of short-circuit current

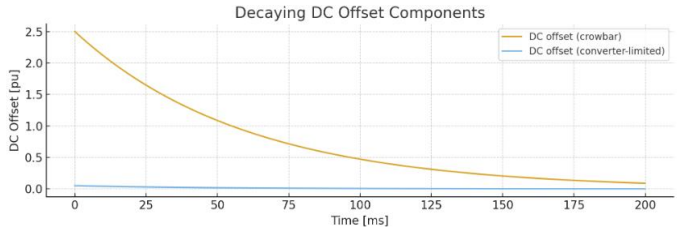

c. Decaying DC Offset Components

Fig.4 Illustration of short-circuit current contribution of DFIG

Fig. 4a: The instantaneous waveform I(t)I(t)I(t) over the time interval (0–40 ms) is shown for two scenarios: converter-limited and crowbar activation.

Fig. 4b: The variation of the current magnitude in the crowbar scenario compared with the converter-limited case.

Fig. 4c: The decay of the DC offset component over time for both scenarios.

The plots in Fig. 4 indicate that: the large initial peak followed by a decay represents induction generator-like behavior when the crowbar is triggered; the initial magnitude in this example is approximately 5 p.u, decaying to about 1.5 p.u (parameters can be adjusted according to actual system data). The DC offset component causes asymmetry in the fault current waveform and decays with a time constant, playing a major role in the peak current IpI_pIp during the first few cycles. In the converter-limited case, the current is approximately equal to the set limit (~1.2 p.u) with very little DC offset.

In the converter-limited mode, the current at the fault location is determined as follows [2], [9]:

$$I_F = I_{grid} + I_{DFIG} \qquad (11)$$

Since the DFIG current is limited to I_{conv_max}, the fault current can be further expressed with a phase angle. If the phase angle is unknown, the DFIG contribution is considered only by its magnitude, $I_{DFIG} = I_{max}$. In this case, the short-circuit current is determined similarly to the formulas presented in Section II.

ISSN No. 2454-6194 | DOI: 10.51584/IJRIAS |Volume X Issue X October 2025

When the crowbar is engaged, the DFIG is modeled as an internal voltage source E_{DFIG} ($\approx U_{ph}$) with an internal impedance Z_{DFIG} (ypically represented as $jX"_m + R_{crowbar}$). The short-circuit current at the fault location is then determined as follows [2], [9]:

$$I_k^{"} = I_{grid} + I_{DFIG} = \frac{E_{grid}}{Z_{grid\_to\_fault}} + \frac{E_{DFIG}}{Z_{DFIG\_to\_fault}} \qquad (12)$$

(Usually, $E_{grid} \approx U_{ph}$, $E_{DFIG} \approx U_{ph}$ if the synchronous/induction machine internal voltage is equivalent to the phase voltage).

The DFIG under crowbar protection can be represented with components $Z_{DFIG}^{(1)}$ và $Z_{DFIG}^{(2)}$; zero-sequence impedance $Z_{DFIG}^{(0)}$ is typically zero or very small (depending on rotor/neutral grounding). When applying phase-to-ground or phase-to-phase short-circuit calculation formulas, the DFIG impedance should be added into the corresponding $Z^{(1)}$ and $Z^{(2)}$.

Impact of Hydro Generators on Short-Circuit Current

When a short circuit occurs, the generator terminal voltage drops abruptly, approaching zero at the fault location (if the fault is close to the generator). The generator current surges to the initial short-circuit current, whose magnitude depends on the machine time constants and internal reactances. The short-circuit current of the generator decays over time with distinct stages:

Subtransient stage: subtransient current (first few cycles, very high due to the small subtransient reactance $X"_d$);

Transient stage: transient current (decays more slowly, governed by the larger transient reactance X'_d);

Steady-state stage: steady-state fault current (much lower, limited by the synchronous reactance X_d).

Therefore, a hydro generator contributes a very large current in the first few cycles following the fault, which may reach 5–7 times the rated current [3].

Due to electromechanical and governor dynamics, the terminal voltage decreases while the fault current remains high. This causes the electromagnetic torque of the generator to drop sharply, whereas the mechanical torque from the water turbine remains unchanged in the short term. As a result, the generator accelerates (rotor angle δ increases). This behavior can be addressed by the block diagram representing the generator control system response, as shown in Fig. 5 [4], [6], [7].

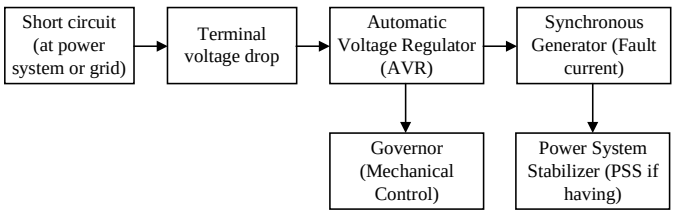

Fig.5 Generator control response during short circuit

The AVR/Exciter receives the input signal (voltage reference) and compares it with the terminal voltage feedback from the generator, then adjusts the excitation accordingly. The synchronous generator contributes to the short-circuit current, leading to a terminal voltage drop and changes in power/speed. The governor receives the power/speed feedback from the generator and regulates the mechanical input (hydraulic turbine). The PSS (Power System Stabilizer) processes the power oscillation signals from the generator and provides a stabilizing signal back to the AVR.

If the fault is prolonged, the short circuit may cause loss of synchronism with the grid. The governor, due to its inertia and slow response, cannot immediately adjust the water flow into the turbine [4], [6], [7].

ISSN No. 2454-6194 | DOI: 10.51584/IJRIAS |Volume X Issue X October 2025

If the fault is cleared quickly (within a few cycles), the generator can remain synchronized and restore its terminal voltage. However, if the fault persists or is cleared too slowly, there is a risk of rotor angle instability and generator disconnection from the system. The fault current waveform contributed by the hydro generator is illustrated in Fig. 5 [4], [6], [7].

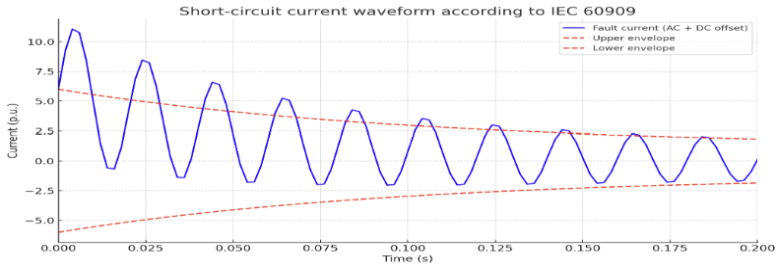

Fig.6 Fault current waveform of the hydro generator

In this figure: the blue curve represents the total short-circuit current, consisting of an AC component with decaying amplitude and a DC offset component that gradually diminishes. The red dashed curve shows the maximum and minimum envelope of the voltage/current waveform over time.

Accordingly, the fault current exhibits a strong DC offset and very high magnitude during the first few cycles. Then, the oscillations gradually decay toward the steady-state level. In the subtransient stage, the current is extremely large immediately after the fault (≈ 5–7 times the rated current), followed by a very rapid decay within the first few cycles. In the transient stage, the current remains above the rated value but decreases more slowly, governed by the transient time constant. In the steady-state stage, the current settles to a smaller value after a long duration (≈ 1.1–1.2 times the norminal current).

For short-circuit calculations, the hydro generator is modeled as an internal emf source $E'' \approx 1\angle 0°$ p.u in series with the subtransient reactance X''_d. Since the hydro generator has the same electrical characteristics as a conventional synchronous generator, the three-phase synchronous machine model can be applied. Typically, the subtransient reactance X''_d is used in fault current studies because the initial stage of the fault current is the most critical.

SIMULATION RESULTS

In the test system, a DFIG plant is connected at Bus 6, while a hydro power plant is connected at Bus 4, as shown in Fig. 7 [11].

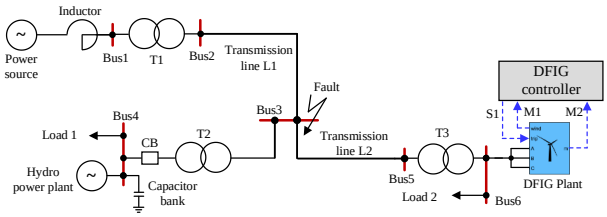

Fig.7 A System with the participation of DFIG and hydro power plant

To evaluate the power distribution across the system introduced in Fig. 7, the simulation parameters are presented in the following tables. These parameters characterize the power sources, inductors, transformers T1, T2 and T3, electrical loads, the DFIG, and the transmission line L1 and L2, small hydro power plant.

Parameters Of Power Source And Inductor

Number	Name of parameter	Symbol	Value
1	Voltage amplitude	$U_{ph\text{-}ph}$	120 kV
2	Frequency	f	60 Hz

ISSN No. 2454-6194 | DOI: 10.51584/IJRIAS |Volume X Issue X October 2025

3	Positive-sequence resistance of inductor	R_1	0.1 Ω
4	Positive-sequence capacitance of inductor	L_1	3×10^4 H
5	Zero-sequence resistance of inductor	R_0	0.3 Ω
6	Zero-sequence capacitance of inductor	L_0	9×10^4 H

Parameters of T1 transformer

Number	Name of parameter	Symbol	Value
1	Norminal power	S_n	50 MVA
2	Voltage ratio	$U_{primary}/U_{secondary}$	120kV/25kV
3	Primary and secondary winding resistance	R	2.67×10^{-3} (p.u)
4	Primary and secondary winding capacitance	L	0.08 (p.u)

Parameters of T2 transformer

Number	Name of parameter	Symbol	Value
1	Rated power	S_{rated}	2.5 MVA
2	Voltage ratio	$U_{primary}/U_{secondary}$	25kV/2.3kV
3	Primary winding resistance	$R_1=R_2$	1.3×10^{-3} (pu)
4	Primary winding inductance	$L_1=L_2$	0.04 (pu)

Parameters of T3 transformer

Number	Name of parameter	Symbol	Value
1	Rated power	S_{rated}	12 MVA
2	Voltage ratio	$U_{primary}/U_{secondary}$	25kV/575V
3	Primary and secondary winding resistance	$R_1=R_2$	8.3×10^{-4} (pu)
4	Primary winding inductance	$L_1=L_2$	0.025 (pu)

Parameters of electric loads

Number	Name of parameter	Symbol	Value
1	Load 1	$P_{Load1}+jQ_{Load1}$	0,2+j0 MVA
2	Load 2	$P_{Load2}+jQ_{Load2}$	1+j0 MVA

ISSN No. 2454-6194 | DOI: 10.51584/IJRIAS |Volume X Issue X October 2025

Parameters of DFIG

Number	Name of parameter	Symbol	Value
1	Number of generator	n	06
2	Rated power	P_{rated}	1.5 MVA
3	Rated voltage	U_{ph-ph}	575 V
4	Power factor	cosφ	0.9
5	Rated frequency	f	60 Hz
6	Rated wind speed	v_{rated}	12 m/s
7	Cut-in wind speed	v_{cut-in}	3 m/s
8	Cut-out wind speed	v_{cut-in}	60 m/s

Parameters of transmission line

Number	Name of parameter	Symbol	Value
1	Length	L_1 and L_2	L_1=18 km; L_2=15 km
2	Positive resistance	R_1	0.1153 Ω/km
3	Zero resistance	R_0	0.413 Ω/km
4	Positive Inductance	X_1	1.05×10^{-3} H/km
5	Zero Inductance	X_0	3.32×10^{-3} H/km
6	Positive Capacitance	C_1	11.33×10^{-9} F/km
7	Zero Capacitance	C_0	5.01×10^{-9} F/km

Parameters of hydro power plant

Number	Name of parameter	Symbol	Value
1	Norminal power	S_n	1.68 MVA
2	Power factor	pf	0.93
3	Norminal voltage	U_n	2.3 kV
4	Stator resistance	R_1	0.0092 p.u
5	Stator inductance	L_1	0.0717 p.u
6	Rotor resistance	R_2	0.007 p.u
7	Rotor inductance	L_2	0.0717 p.u

ISSN No. 2454-6194 | DOI: 10.51584/IJRIAS |Volume X Issue X October 2025

8	Inertia constant	H	0.5 s
9	Friction factor	F	0

The wind speed variation scenario is illustrated in Fig. 8.

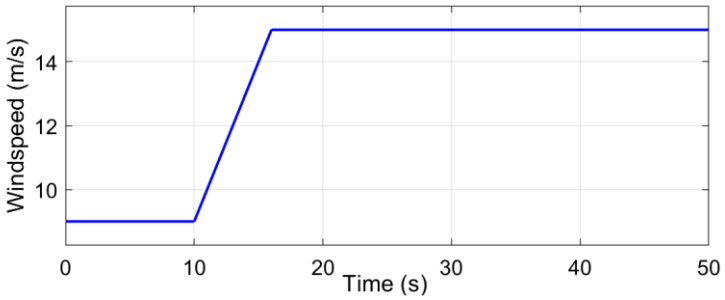

Fig.8 Wind speed variation scenario

The simulation study considers three operating scenarios: (i) normal operation without faults, (ii) a temporary short-circuit on Line 2 near Bus 3 at 6 s lasting 0.1 s, and (iii) a sustained short-circuit on Line 2 near Bus 3 at 6 s lasting 0.9 s.

Simulation results for Scenario 1: Fault-free system

The corresponding DFIG active and reactive power responses under Scenario 1 (no fault) are shown in Fig. 9.

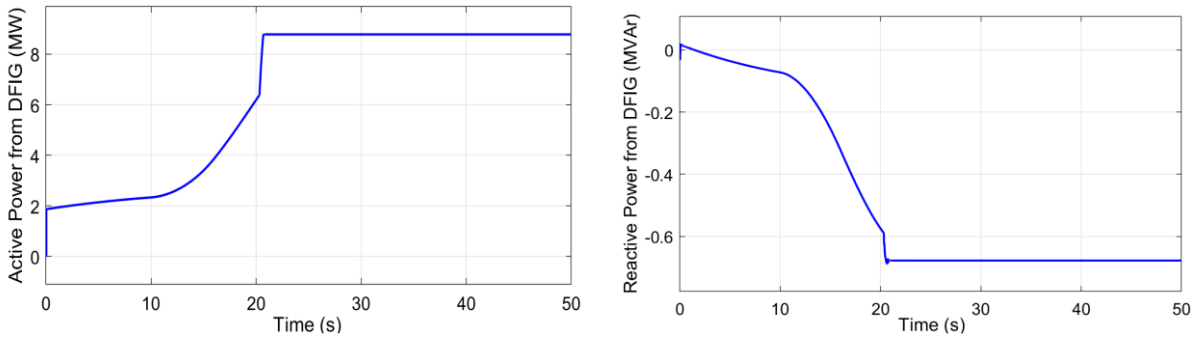

a. Active power b. Reactive power

Fig.9 Active and reactive power output from the DFIG in Scenario 1

The active and reactive power of the small hydro generator are illustrated in Fig. 10.

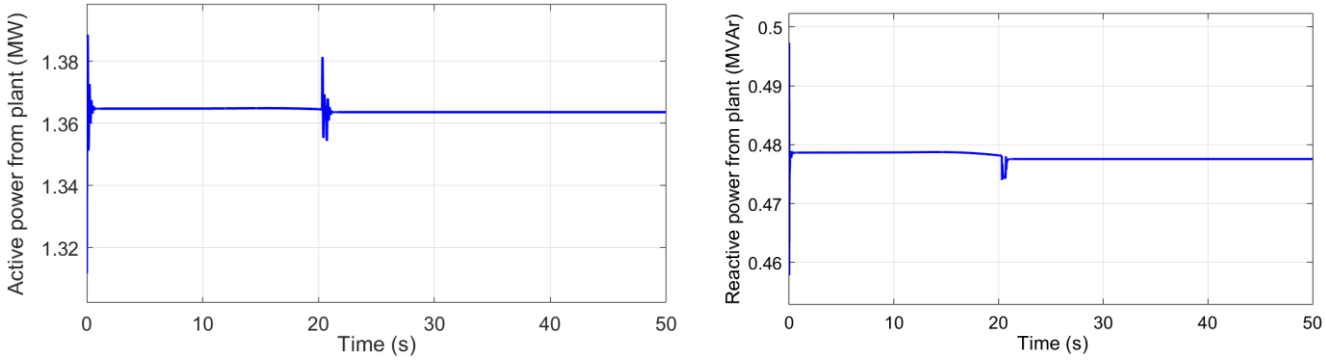

a. Active power b. Reactive power

Fig.10 Active and reactive power output of the small hydro generator in Scenario 1

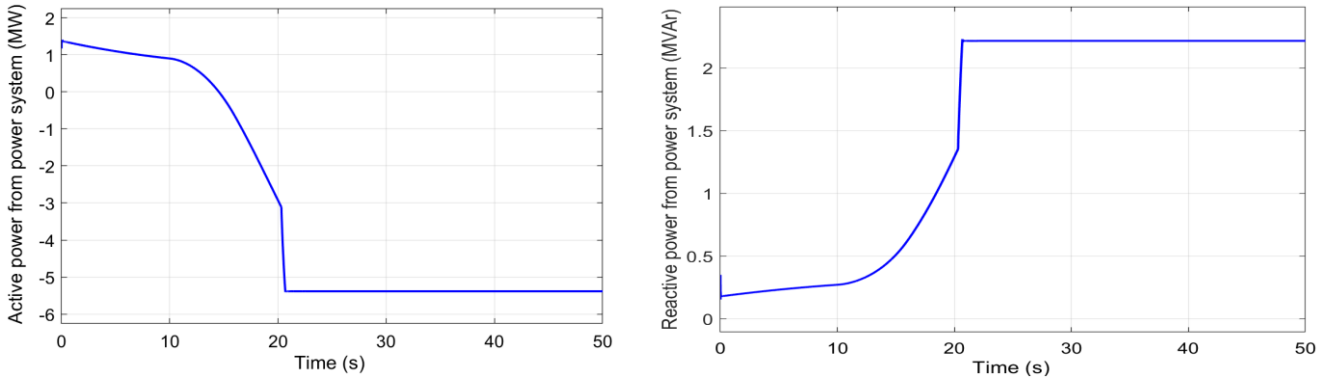

a. Active power b. Reactive power

Fig.11 The active and reactive power exchanged with the power source in Scenario 1

The simulation results show that the power output from the DFIG and the hydro generator remains positive (both active and reactive power). Meanwhile, the active power exchanged with the grid is positive during the initial stage and becomes negative in the steady state, whereas the reactive power remains positive throughout. This indicates that both the DFIG and the hydro generator supply active power to the system while absorbing reactive power to maintain voltage stability. The power distribution in Scenario 1 is presented in Fig. 12.

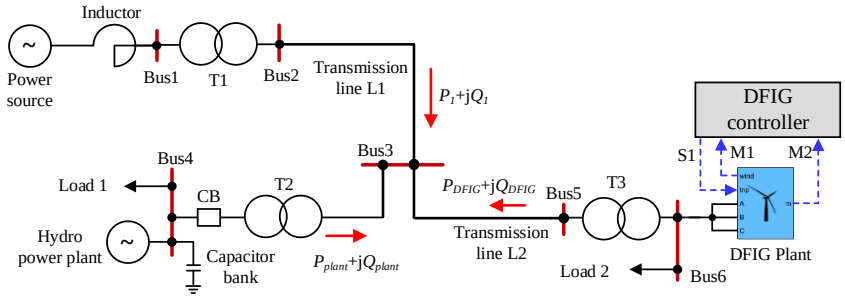

Fig.12 Power distribution in Scenario 1

The simulation results of current exchanged with the grid are shown in Fig. 13, the current output of the hydro generator in Fig. 14, the current output of the DFIG in Fig. 15, and the current through Bus 3 in Fig. 16.

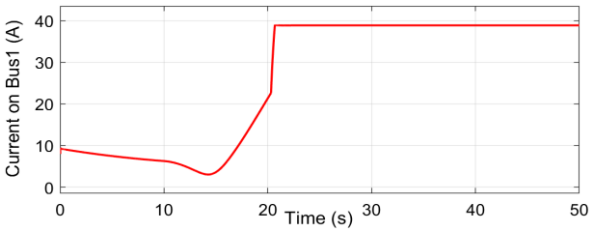

Fig.13 Current exchanged with the grid in Scenario 1

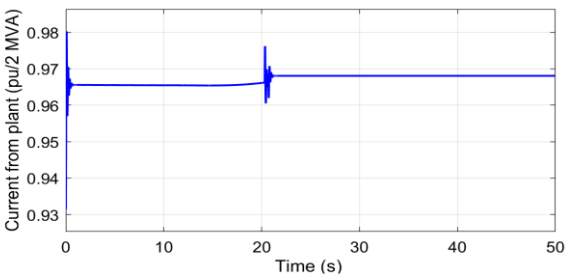

Fig.14 Current from the hydro plant to Bus 3 in Scenario 1

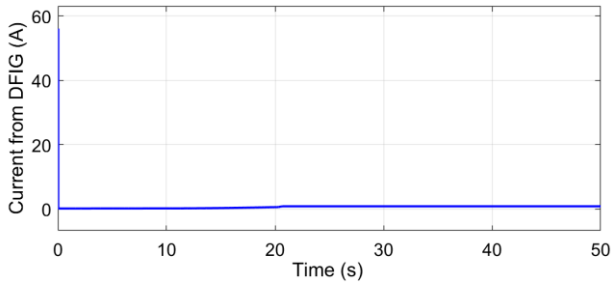

Fig.15 Current from the DFIG to Bus 3 in Scenario 1

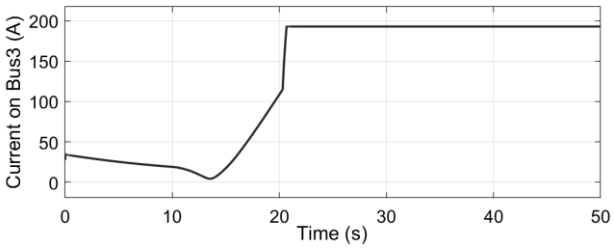

Fig.16 Current through Bus 3 in Scenario 1

It can be observed that the current exchanged with the grid and the current through Bus 3 have similar waveforms, differing only in magnitude due to the voltage level difference and the power losses on transmission line L1.

Scenario 2: Single-phase-to-ground fault lasting 0.1 s

The simulation results for Scenario 2 (single-phase-to-ground fault of 0.1 s) regarding the grid current, hydro generator current, DFIG current, and Bus 3 current are presented in Fig. 17–20.

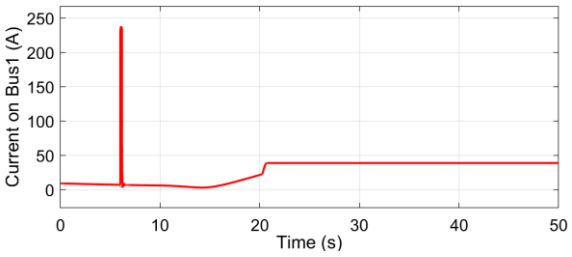

Fig.17 Current exchanged with the grid in Scenario 2

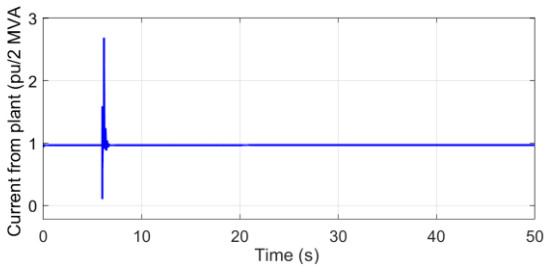

Fig.18 Current from the hydro generator in Scenario 2

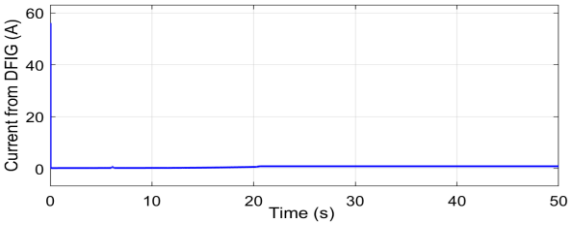

Fig.19 Current from the DFIG in Scenario 2

ISSN No. 2454-6194 | DOI: 10.51584/IJRIAS |Volume X Issue X October 2025

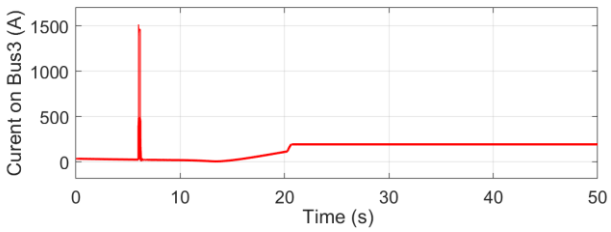

Fig.20 Current through Bus 3 in Scenario 2

Scenario 3: Three-phase-to-ground fault lasting 0.1 s

Fig. 21–24 present the simulation results of Scenario 4, i.e., a three-phase-to-ground fault of 0.1 s, including the grid current, hydro generator current, DFIG current, and the current through Bus 3.

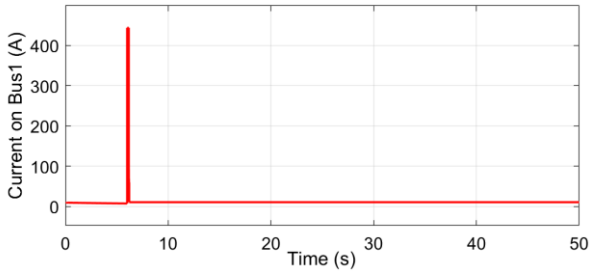

Fig.21 Current exchanged with the grid in Scenario 3

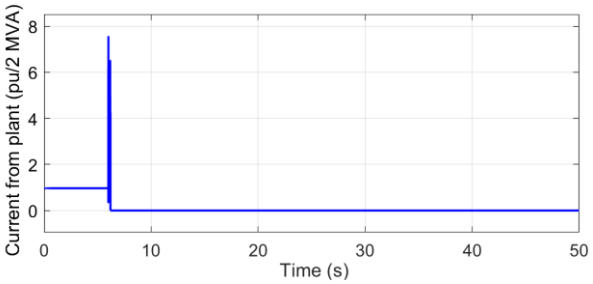

Fig.22 Current from the hydro generator in Scenario 3

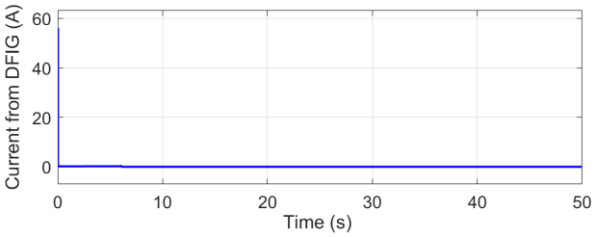

Fig.23 Current from the DFIG in Scenario 3

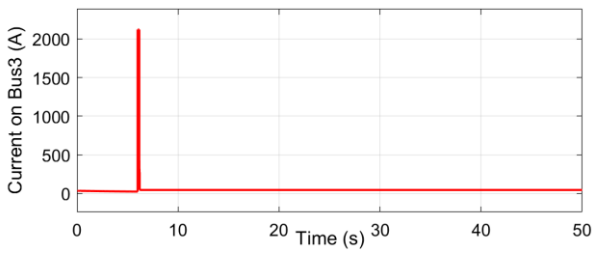

Fig.24 Current through Bus 3 in Scenario 3

The simulation results for Scenarios 2 and 3 show that the fault currents from the power source, hydro generator, and DFIG surge at t=6 s. The hydro generator exhibits a different transient response compared with the power

source and the DFIG, due to the influence of the excitation system. Since the fault is cleared at t=6.1, the protection of the hydro generator and DFIG is not triggered. These results accurately reflect the transient behavior of system components under temporary faults.

Scenario 4: Single-phase-to-ground fault lasting 1 s

Fig. 25–28 present the simulation results of Scenario 4, i.e., a single-phase-to-ground fault of 0.9 s, including the grid current, hydro generator current, DFIG current, and the current through Bus 3.

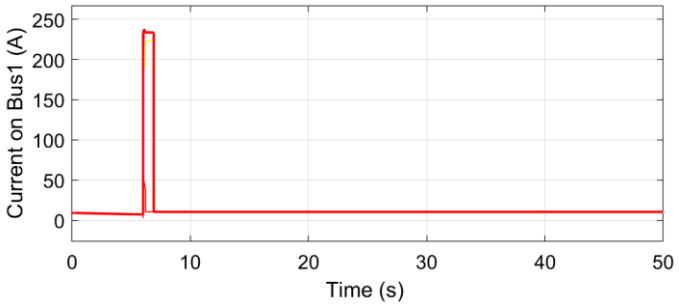

Fig.25 Current exchanged with the grid in Scenario 4

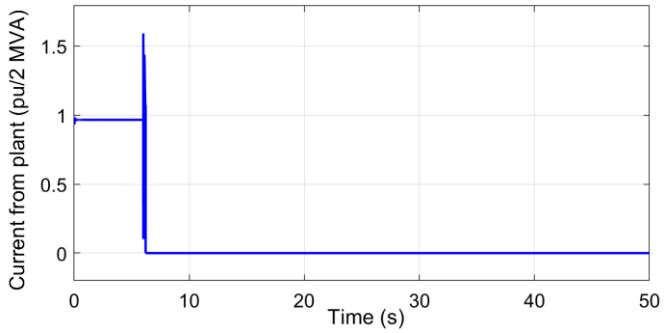

Fig.26 Current from the hydro generator in Scenario 4

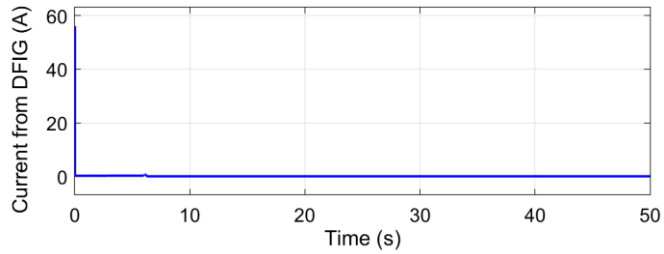

Fig.27 Current from the DFIG in Scenario 4

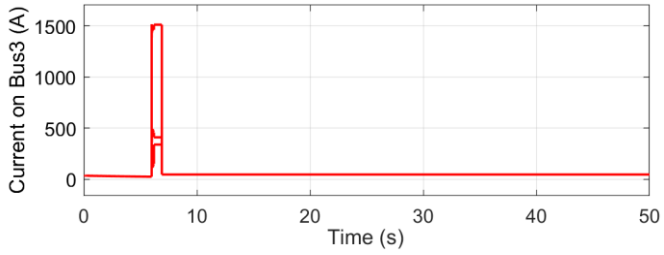

Fig.28 Current through Bus 3 in Scenario 4

Scenario 5: Three-phase-to-ground fault lasting 1 s

Fig. 29–32 present the simulation results of Scenario 5, i.e., a three-phase-to-ground fault of 0.9 s, including the grid current, hydro generator current, DFIG current, and the current through Bus 3.

ISSN No. 2454-6194 | DOI: 10.51584/IJRIAS |Volume X Issue X October 2025

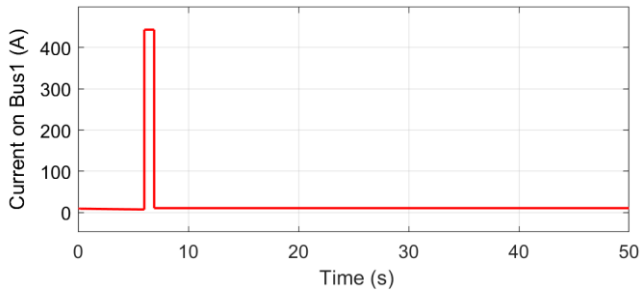

Fig.29 Current exchanged with the grid in Scenario 5

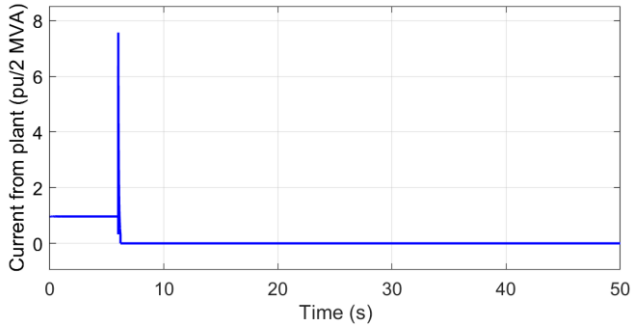

Fig.30 Current from the hydro generator in Scenario 5

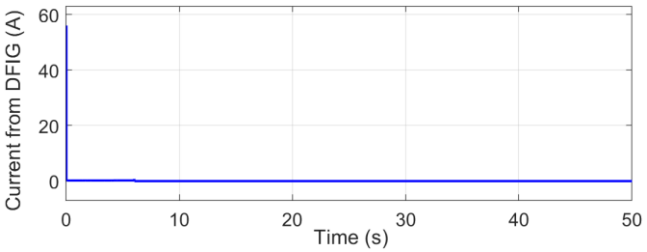

Fig.31 Current from the DFIG in Scenario 5

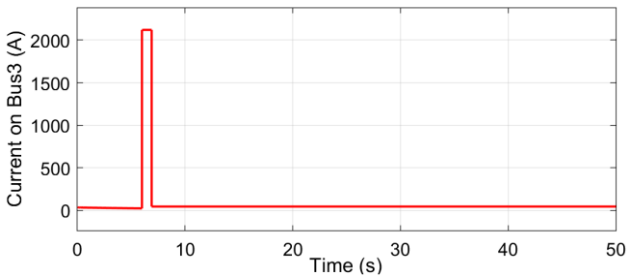

Fig.32 Current through Bus 3 in Scenario 5

The results for Scenarios 4 and 5 indicate that the short-circuit currents from the power source, hydro generator, and DFIG surge at t=6 s and last until t=6.9 s. Both the hydro generator and the DFIG cease power generation after the fault due to the governor triggering the disconnection of circuit breakers from the system. Although the fault is cleared at t=6.9 s, both generators remain disconnected, so the power source supplies the load. This reflects the system behavior under sustained faults, including both single-phase and three-phase short-circuits.

CONCLUSIONS

The main contribution of this paper is the successful simulation and analysis of short-circuit currents in a power system that simultaneously integrates a small hydro generator and a DFIG-based wind plant. The system configuration and the DFIG control structure are detailed, including the use of power electronic converters for controlling rotor-side and grid-side power flows. Several fault scenarios were established, including faults at buses

connected to the DFIG and hydro generator, to evaluate the transient current responses and the ability of different generators to support the system.

The results show that the fault current contribution from the hydro generator is large in the initial stage and decays according to the subtransient, transient, and steady-state time constants, consistent with synchronous generator characteristics. In contrast, the fault current from the DFIG is limited by the converter and crowbar protection mechanism, with its behavior depending on the control strategy and LVRT mode. This highlights the distinct contributions of the two generation types to short-circuit currents.

Such analysis and comparison accurately reflect the distribution of power, current magnitude, and phase at system nodes, thereby providing a comprehensive view of system responses under fault conditions. These findings offer system operators a technical basis for evaluating stability margins and for determining generation dispatch or load-shedding strategies under severe contingencies.

The contributions of this study can be extended in future work by considering more complex fault scenarios, such as faults within the DFIG itself, multiple simultaneous faults in weak grids, or coordination among multiple distributed generators. Such analyses will further enhance the reliability and stability of modern power systems with high penetration of renewable energy sources.

ACKNOWLEDGMENTS

This study is completely supported by Thai Nguyen University of Technology, Thai Nguyen University, Viet Nam.

REFERENCES

1. J. Yin, “Improved Short-Circuit Current Calculation of Doubly Fed Wind Turbines With Uninterrupted Excitation,” Frontiers in Energy Research, vol. 9, 2021. Frontiers
2. F. Xiao, Y. Xia, K. Zhang, Z. Zhang, and X. Yin, “Short-circuit model of the DFIG considering coordinated control strategy of grid- and rotor-side converters,” Electric Power Systems Research, vol. 202, 2022. ScienceDirect
3. A. Arastou, “Parameter identification of small distributed hydro generators under sudden short circuit test,” IET Generation, Transmission & Distribution, vol. 16, issue not., 2022. IET Research Journals
4. D. Brankovic and F. Schuerhuber, “Short-circuit current of a hydropower plant with consideration of constant switching and fault arc voltages,” IET Generation, Transmission & Distribution, 2024. IET Research Journals+1
5. J. Yin, “A New Short-Circuit Current Calculation and Fault Analysis Model for Doubly Fed Induction Generator,” PMC, 2023. PMC
6. R. He, “Calculation method of external fault short-circuit current for variable-speed pumped storage units,” Frontiers in Energy Research, 2023. Frontiers
7. A. Gozdowiak and M. Antal, “Inter-Turn Short Circuits in Stator Winding of Permanent Magnet Synchronous Generator Dedicated for Small Hydroelectric Power Plants,” Energies, vol. 18, no. 14, 2025. MDPI
8. J. Yin, “Influence of Reactive Power Support Control Strategy on Short-Circuit Current Calculation and Fault Analysis Method of DFIG,” Frontiers in Energy Research, 2021. ADS
9. J. Yin et al., “Short Circuit Current Analysis Of DFIG-Type Wind Generator with Crowbar Action,” (conference / preprint) 202x. Bohrium
10. C. Geiger et al., “Power Plant Transients including Hydraulic Short Circuit in Hydro Power Plant,” Energies, 2023. MDPI
11. Richard Gagnon, Bernard Saulnier, Alain Forcione (Hydro-Quebec), https://www.mathworks.com/help/sps/ug/wind-farm-dfig-phasor-model.html